Video Article

Optogenetic Functional MRI

Peter Lin[1], Zhongnan Fang[2], Jia Liu[1], Jin Hyung Lee[1,2]

[1]Neurology and Neurological Sciences, Stanford University

[2]Electrical Engineering, Neurology and Neurological Sciences, Stanford University

Correspondence to: Jin Hyung Lee at ljinhy@stanford.edu

Abstract

The investigation of the functional connectivity of precise neural circuits across the entire intact brain can be achieved through optogenetic functional magnetic resonance imaging (ofMRI), which is a novel technique that combines the relatively high spatial resolution of high-field fMRI with the precision of optogenetic stimulation. Fiber optics that enable delivery of specific wavelengths of light deep into the brain *in vivo* are implanted into regions of interest in order to specifically stimulate targeted cell types that have been genetically induced to express light-sensitive trans-membrane conductance channels, called opsins. fMRI is used to provide a non-invasive method of determining the brain's global dynamic response to optogenetic stimulation of specific neural circuits through measurement of the blood-oxygen-level-dependent (BOLD) signal, which provides an indirect measurement of neuronal activity. This protocol describes the construction of fiber optic implants, the implantation surgeries, the imaging with photostimulation and the data analysis required to successfully perform ofMRI. In summary, the precise stimulation and whole-brain monitoring ability of ofMRI are crucial factors in making ofMRI a powerful tool for the study of the connectomics of the brain in both healthy and diseased states.

Video Link

The video component of this article can be found at https://www.jove.com/video/53346/

Introduction

Optogenetic functional magnetic resonance imaging (ofMRI) is a novel technique that combines the spatial resolution of high-field fMRI with the precision of optogenetic stimulation[1-11,38], enabling cell type-specific mapping of functional neural circuits and their dynamics across the whole brain. Optogenetics allows for specific cell types to be targeted for stimulation by the introduction of light-sensitive trans-membrane conductance channels, called opsins. Specific elements of neural circuits are genetically modified to express these channels, enabling millisecond-timescale modulation of activity in the intact brain[1-15]. fMRI provides a non-invasive method of determining the brain's global dynamic response to optogenetic stimulation of specific neural circuits through measurement of the blood-oxygen-level-dependent (BOLD) signal[16-18], which provides an indirect measurement of neuronal activity.

The combination of these two techniques, termed optogenetic functional magnetic resonance imaging (ofMRI), is advantageous over other methods of recording brain activity during stimulation such as electrophysiology because it can provide a view of the entire brain at relatively high spatial resolution. This enables the detection of neuronal activity in response to targeted stimulation at great distances from the site of stimulation without the need for implantation of invasive recording electrodes[1-11]. ofMRI is advantageous over the more traditional method of performing electrical stimulation during fMRI, which can recruit different cell types near the electrode and thus confound the causal influence of each population[19]. In addition, the electrodes used for electrical stimulation and the generated current can produce artifacts during MR imaging[20]. Indeed, ofMRI enables the observation of the influence on global brain activity from the specific modulation of a wide variety of cell types through the use of advanced genetic targeting techniques such as the Cre-Lox system in transgenic animals or the use of promoters. Combinatorial optical control with whole-brain monitoring is possible with ofMRI through the use of both NpHR to inhibit and ChR2 to excite specific cell types. The optogenetic toolkit available for use in ofMRI is also rapidly improving over time with the introduction of opsins with increased light-sensitivity or improved kinetics, of stabilized step function opsins (SSFOs) or of red-shifted opsins that may negate the requirement for implanted fiber optics, enabling non-invasive stimulation during imaging[21]. These possibilities are not available with electrical stimulation.

However, signal artifacts resulting from tissue heating due to light delivery in the brain have been reported[22], where temperature-induced modification of relaxation times has been shown to produce pseudo activation. Researchers performing ofMRI should therefore be aware of this potential confound. With the proper setup and controls, the issue can be addressed. Additionally, relatively low temporal resolution of measuring the hemodynamic response in fMRI may be a limiting factor for certain applications of this technique.

This protocol first describes the construction of the fiber optic implants that enable delivery of specific wavelengths of light deep into the brain *in vivo*. The protocol then describes the delivery of the opsin-encoding viral vector to a precise brain region using stereotactic surgery. Next

the protocol describes the process of whole-brain functional MRI during simultaneous light stimulation. Finally, the protocol outlines basic data analysis of the acquired data.

Of note, the optogenetics described here require a chronic implant for light delivery. However, the fiber optic implants are stable and bio-compatible, allowing for longitudinal scanning and investigation of neural circuitry over a period of months[23,24].

In summary, the precise stimulation and whole-brain monitoring ability of ofMRI are crucial factors in making ofMRI a powerful tool for the study of the connectomics of the brain. In addition, it can provide novel insight into the mechanisms of neurological diseases[25] when coupled with different animal models. Indeed, ofMRI has been used to elucidate the network activity of distinct hippocampal subregions associated with seizures[8]. Therefore, laboratories interested in answering systems-level neuroscience questions will find this technique of importance.

Protocol

Ethics Statement: Experimental procedures here have been approved by the Stanford University Institutional Animal Care and Use Committee (IACUC).

1. Preparing Patch Cables and Ferrule Implants

Note: Although patch cables and ferrule implants are available commercially, producing these in-house enables specialty designs and will cost less.

1. To prepare a fiber patch cable for delivering light from the laser to the implant in the brain, first cleave the optical fiber to the desired length.
    1. Using a fiber cleaver, terminate the optical fiber to produce a flat end at the termination point. If the fiber has been coated with a jacket, strip the jacket off with a fiber-stripping tool beforehand.
    2. Cleave the other end of the optical fiber to produce the desired length for the cable, ensuring that the cable is long enough to extend from the light source to the animal inside the bore of the scanner.
2. Mix a small amount of epoxy glue in a 1:1 ratio onto a piece of aluminum foil shortly before the next step, as the epoxy glue becomes too viscous for use 5 min after mixing.
3. Using a small wooden stick, gently apply epoxy glue to the part of the fiber that will be placed inside the concave side of the ceramic ferrule and then apply a small drop onto the surface of the flat side of the ferrule. After inserting it into the ferrule, ensure that a small length of fiber (<0.5 mm) protrudes from the flat side of the ceramic ferrule. Allow the epoxy glue to harden O/N for optimal results.
4. On the side of the fiber optic patch cable that will connect to the laser light source, gently apply epoxy glue to the part of the fiber that will be placed inside the concave side of the ferrule of the FC/PC connector and then apply a small drop onto the surface of the flat side of the ferrule. After inserting it into the ferrule, ensure that a small length of fiber (<0.5 mm) protrudes from the flat side of the ferrule. Allow the epoxy glue to harden O/N for optimal results.
5. Polish the flat end of the ferrules for both sides of the cable using a polishing disk by using tweezers to apply gentle downward pressure on the ferrule while making figure-8 rotations on aluminum oxide lapping sheets (from 3 µm to 1 µm to 0.3 µm grit).
6. Examine the flat end of the ferrule with a microscope at 100X magnification. Ensure that the surface of the flat end, including the fiber optic surface itself, is free of any epoxy glue; continue polishing if epoxy glue remains on the surface. Ensure that the fiber optic surface has not broken or chipped.
   CAUTION: Ensure personnel take appropriate laser safety training classes and wear laser safety goggles before handling laser equipment.
7. Connect the fiber optic patch cable to the laser light source through the FC/PC connector and align the fiber tip to the focal point of the coupler. Measure the light transmission power of the fiber with a power meter to ensure adequate light output.
   Note: The following steps are for preparing ceramic ferrules with fiber optics for chronic implantation into the brain; ceramic ferrules are hollow in the center and carry fiber optics to deliver light from a patch cable to a region of interest (ROI) within the brain.
8. Using a fiber cleaver, terminate the optical fiber to produce a flat end at the termination point. If the fiber has been coated with a jacket, strip the jacket off with a fiber-stripping tool beforehand.
9. Cleave the other end of the optical fiber to produce the desired length for implantation into the brain. Determine the length of the fiber using a stereotaxic atlas to target the ROI within the brain.
    1. For example: to target dorsal hippocampus in rat which is 3.5 mm below bregma, ensure that the length of the fiber protruding from the ferrule is 3.5 mm + 0.25 mm, accounting for skull thickness and allowing for margin of error. Therefore, check that the final length of the fiber is 3.5 mm + 0.25 mm + 10.5 mm (length of the ferrule) = 14.25 mm.

10. Mix a small amount of epoxy glue in a 1:1 ratio onto a piece of aluminum foil shortly before the next step (the epoxy glue becomes too viscous for use 5 min after mixing).
11. Using a small wooden stick, gently apply epoxy glue to the part of the fiber that will be placed inside the concave side of the ceramic ferrule and then apply a small drop onto the surface of the flat side of the ferrule. After inserting it into the ferrule, ensure that a small length of fiber (<0.5 mm) protrudes from the flat side of the ceramic ferrule. Allow the epoxy glue to harden O/N for optimal results.
12. Polish the flat end of the ferrule using a polishing disk by using tweezers to apply gentle downward pressure on the ferrule while making figure-8 rotations on aluminum oxide lapping sheets (from 3 µm to 1 µm to 0.3 µm grit).
13. Examine the flat end of the ferrule with a microscope at 100X magnification. Ensure that the surface of the flat end, including the fiber optic surface itself, is free of any epoxy glue; continue polishing if epoxy glue remains on the surface. Ensure that the fiber optic surface has not broken or chipped.
14. Couple the polished ferrule to a fiber optic patch cable with a ferrule sleeve and connect the patch cable to a laser light source. Measure the light transmission power at the tip of the fiber with a power meter to ensure adequate efficiency.
15. Keep a log of the power output required from the patch cable's ferrule for each ferrule implant to output the desired power level at the tip of the fiber optic (2.5 mW in this protocol). Discard ferrules with an attenuation rate of over 50% and with non-circular output pattern.

2. Stereotaxic Implantation Surgery and Virus Injection

1. Ensure that any experimental procedures involving the use of animals are approved by the local IACUC. Maintain aseptic conditions during survival surgeries by following aseptic procedures, including using sterile gloves, sterile masks, sterile surgical drapes and sterilized surgical instruments.
CAUTION: Ensure that surgeons are wearing proper personal protective equipment (PPE) including safety goggles before beginning the procedure. Follow standard biosafety procedures when working with adeno-associated vector (AAV), taking care to avoid splashing. Dispose of AAV waste in a biohazard container.
2. Load a microliter syringe with enough AAV for injection into the animal plus extra to account for potential volume losses (total of 4 µl per animal), keeping the syringe on ice before use. In this protocol, AAV5-CaMKIIa-hChR2(H134R)-EYFP at a titer of 4×10^{12} vg/ml is used. Place the animal under isoflurane anesthesia with an induction chamber, connected to a precision isoflurane vaporizer set at 3 - 4% with an oxygen gas source.
3. Shave the head with an electric razor and perform a triple surgical scrub on the skin using betadine and a 70% ethanol rinse.
4. Once the animal is in deep anesthesia (check toe reflex and breathing rate), immobilize the animal's skull in a stereotaxic apparatus with intra-aural positioning studs and tooth bar.
Note: The entire procedure will take 1 - 2 hr, from anesthesia induction to recovery.
5. Set the anesthesia to an appropriate level (1 - 3% isoflurane on the vaporizer) and continually monitor the animal's vital signs, adjusting anesthesia as necessary to maintain a breathing rate of ~40 breaths/min. Administer ophthalmic ointment on the eyes of the animal to prevent dryness while under anesthesia.
6. Make a 15 - 20 mm midline scalp incision with a scalpel and retract the scalp using surgical hemostats attached to the periosteum. Reference lambda and bregma to position the drill bit over the coordinates for the ROI.
7. Drill a small craniotomy (2 - 3 mm) over the ROI with a dental drill, taking care not to puncture the brain. Slowly insert needle attached to the microliter syringe through the craniotomy to the ROI in the brain.
8. With a microsyringe pump controller, inject 2 µl of the vector solution into the ROI. Use a flow rate of 150 nl/min to avoid tissue damage. After the injection is complete, wait 10 min before removing the syringe slowly, at a rate of 0.5 mm/min.
9. Following injection, dry the surface of the skull. Reference lambda and bregma to confirm coordinates and then insert the ferrule implant to the target depth (for example: 3.5 mm below bregma for dorsal hippocampus) at a rate of about 0.5 mm/min. Mount the ferrule implant to the skull using dental cement. After the dental cement has solidified, seal the incision with sutures (size 5-0 for rats) around the dental cement cap.
10. After surgery, place the animal in its cage singly housed with half of the cage on top of a heater for anesthesia recovery. Do not leave an animal unattended until it has regained sufficient consciousness to maintain sternal recumbency. Do not place the animal in the company of other animals until it has fully recovered.
11. For post-surgical management of pain, administer buprenorphine subcutaneously every 12 hr at a dosage of 0.05 mg/kg for 24 hr. Administer antibiotic powder daily over the incision site for 3 days.
12. Remove the sutures approximately two weeks after the surgery to prevent scabbing.
13. Wait 4 - 6 weeks after the virus injection for sufficient expression of optogenetic genes before performing experiments.

3. Optogenetic Functional MRI

CAUTION: Exercise caution around the permanent magnetic field of an MRI scanner. Secure equipment, including the function generator, light source, ventilator, capnograph and gas tanks, sufficiently far away (at least beyond the 5 Gauss limit).

1. Place the animal under gas anesthesia with an induction chamber, connected to a precision isoflurane vaporizer set at 5% with an oxygen gas source.
2. Once the animal is in deep anesthesia (check toe reflex and breathing rate), intubate the animal according to the protocol detailed in Rivard *et al.* (2006) to allow monitoring of carbon dioxide by capnography[26]. Note: intubation is critical in maintaining proper levels of expiratory CO_2 during imaging.
3. Secure the animal in the scanner cradle.
Note: In this protocol, the cradle was custom produced but such cradles are also commercially available. The rat cradle functions to secure the animal within the scanner for delivery of anesthesia, heated air and for restriction of motion.
4. Deliver a mix of isoflurane (ranging from 1.2 - 1.5%) in approximately 60% nitrous oxide and 40% oxygen via tubing through the cradle. Ensure that the animal's head is securely fixed in order to avoid motion artifacts.
5. Provide heated air through tubing in the cradle and insert a rectal thermometer with lubricant to monitor body temperature. Administer ophthalmic ointment on the eyes of the animal to prevent dryness while under anesthesia.
6. Connect the fiber optic patch cable to a laser light source and measure the output at the tip of the patch cable's ferrule with a power meter.
7. Adjust to the appropriate power level (determined previously in step 1.15) to produce the desired output (2.5 mW in this protocol) at the tip of the fiber optic implanted inside the brain. Since excessive power output from the fiber optic can potentially cause tissue damage inside the brain or cause tissue heating that will produce signal artifacts, do not significantly increase the power output of the laser beyond the intended output.
8. Prevent light leakage from the implant with a cone of black electrical tape and cover the eyes of the animal. Couple the fiber optic cable to the ferrule implant on the animal with a ferrule sleeve.
9. Place the coil over the head of the animal. Insert the cradle with animal into the bore of the scanner.
Note: In this protocol, the single-loop transmit-receive coil was custom produced and pre-tuned to receive the optimal radio frequency from brain tissue.
10. Monitor breathing rate and body temperature throughout this process, adjusting the artificial ventilator and heater as necessary to keep physiological values within limits (ensure that expiratory CO_2 is 3 - 4% by rotating the knobs on the ventilator to adjust stroke frequency and volume and that temperature is 37 °C by clicking the arrows for temperature setting).

11. Select a positioning sequence to image the animal head location. If the brain is not at the iso-center, adjust the animal head location and repeat the positioning scan until the brain is at the iso-center. Select a linear shimming sequence and click load in the sequence selection window. Next, click start to reduce inhomogeneities of the magnetic field.
    Note: Shimming is a critical step that will directly influence the integrity of the fMRI data.
12. Select a T2-weighted sequence and click load in the sequence selection window. Next, click start to acquire T2-weighted high-resolution coronal anatomical images prior to fMRI to check on the overall integrity of the brain and to confirm the location of the optical fiber implant.
    Note: These images can be used as anatomy overlays for the ofMRI scan series.
13. Connect BNC cables from the triggering port of the MRI scanner to the function generator so that the laser light source is driven according to an experimental stimulation paradigm.
    Note: In this protocol, the stimulation paradigm is 30 sec of baseline followed by 20 sec on/40 sec off for six min.
14. Select a multi-slice gradient recalled echo (GRE) sequence and click load in the sequence selection window. Next, click start to acquire 35 mm x 35 mm (2D FOV) in-plane coronal slices with 0.5 mm x 0.5 mm x 0.5 mm spatial resolution.
    Note: The GRE sequence used here has a repetition time (TR) and echo time (TE) of TR/TE = 750/12 msec and a 30° flip angle.
15. At the conclusion of the scan, remove the animal from the scanner and monitor until it has awakened from anesthesia and can maintain sternal recumbency.

4. ofMRI Data Analysis

Note: The following steps are performed in MATLAB as described in a publication on high-throughput ofMRI[27].

1. After the raw scan data has been transferred to the computer used for analysis, use sliding window reconstruction to update the image every TR, with a four-interleave spiral readout, 750 msec TR and 12 msec echo time to acquire 23 slices per scan series. Instead of conventional reconstruction where new fMRI images are reconstructed only after all interleaves are acquired for each slice, the sliding window reconstruction method reconstructs images after the acquisition of each interleaf[27].
2. Process the raw data for two-dimensional gridding reconstruction, motion correction, and calculation of time series as described previously[27].
3. Use a threshold coherence method to determine activated voxels by calculating the percent modulation of the BOLD signal of each voxel relative to the baseline period collected prior to stimulation as described previously[27]. Calculate coherence values as the magnitude of the Fourier transform at the frequency of repeated stimulation cycles divided by the sum-of-squares of all frequency components[8].
4. Using the time-series data for each voxel, average motion-corrected images that belong to consecutive scans of the same stimulation paradigm first. Then align the average 4D images to a common coordinate frame with a six degree-of-freedom rigid body transformation plus isotropic scaling for comparison within and between animals as described previously[27].

Representative Results

Figure 1 and **Figure 2** show representative data resulting from 20 Hz (15 msec pulse width, 473 nm, 30% duty cycle) optogenetic stimulation of the motor cortex. A stimulation paradigm of 30 seconds of baseline followed by 20 sec on/40 sec off for six min was used. Previous studies have shown that this paradigm produces robust BOLD signal from optogenetic stimulation[1,8]. **Figure 1** shows activated voxels detected both at the local site of stimulation (motor cortex) and in the thalamus, as a result of the long-range synaptic connections between these regions. **Figure 2** shows that temporal information can be gleaned from HRFs, as the thalamic response is delayed (lower initial slope) compared to the motor cortex response after optogenetic stimulation.
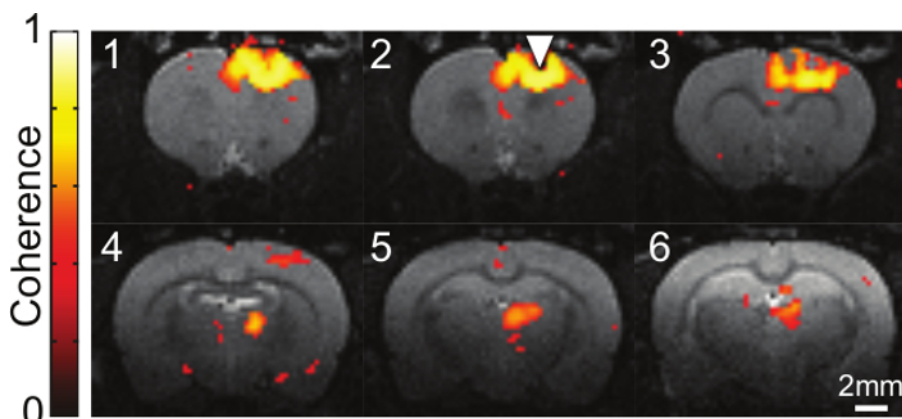

Figure 1. Activation Map of BOLD Signal Induced by Optogenetic Stimulation of CaMKIIa-expressing Cells in Motor Cortex. Coherence values of active voxels, identified as those significantly synchronized to repeated stimulations, are shown overlaid on a T2-weighted coronal anatomical slice. Data collected over a six min, 30 sec period (initial 30 sec baseline and six stimulation cycles of 20 sec on/40 sec off with 473 nm light, 20 Hz, 15 msec pulse width) are condensed into one activation map. Sequential slices are 0.5 mm apart and the location of the fiber optic implant is denoted by the triangle. Please click here to view a larger version of this figure.
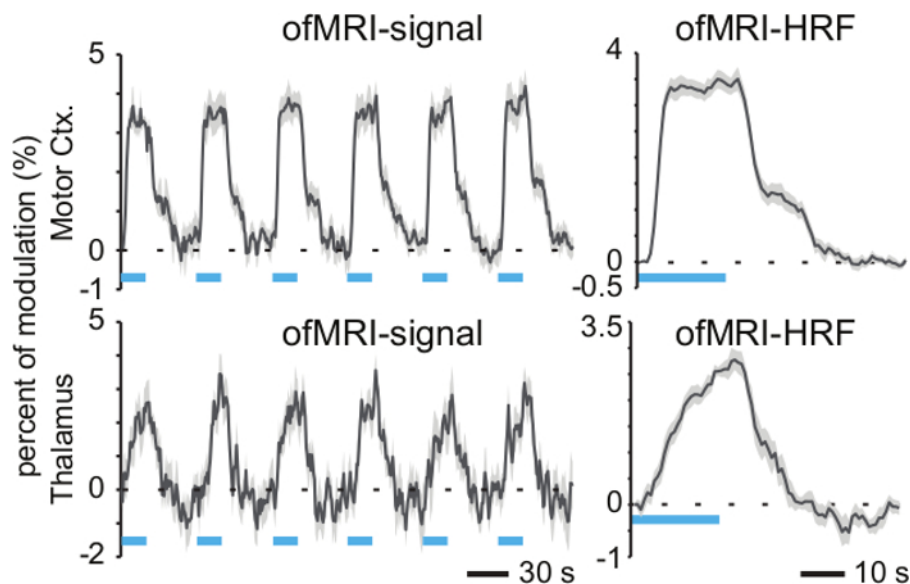
Figure 2. Hemodynamic Response Function. (Left) The percent modulation of the BOLD signal relative to baseline is shown for active voxels in motor cortex and thalamus during optogenetic stimulation of motor cortex (six stimulation cycles of 20 sec on/40 sec off with 473 nm light, 20 Hz, 15 msec pulse width). Shaded grey error bars denote standard error across activated voxels within ROI. (Right) Time-averaged responses are given by the hemodynamic response functions (HRF). The thalamus HRF shows a delayed response relative to the stimulated motor cortex. Blue bars indicate periods of 473 nm photostimulation. Shaded grey error bars denote standard error across six cycles. Please click here to view a larger version of this figure.

Discussion

Motion of the subject during imaging is a significant source of artifact that can lead to data corruption. Appropriately securing the animal on the imaging cradle can minimize such artifacts as will maintaining appropriate anesthesia levels. Here, we used isoflurane but alternative anesthetics, such as medetomidine or ketamine and xylazine, should also be considered. However, the levels and choice of anesthetic can influence many parameters in the brain, including the BOLD response[28]. Isoflurane can cause changes in neuronal excitability[29]. Other anesthetics can also affect GABA synaptic inhibition[30]. Thus, the choice of anesthesia is important when performing ofMRI given its ability to affect neuronal activity. ofMRI in the absence of anesthesia is possible but can be challenging with increased motion from the animal, which can be reduced if the animal is habituated; such awake ofMRI studies have previously been performed and would avoid the confounding effect of anesthesia on the brain[9,10]. Post-processing motion correction algorithms can be used to greatly mitigate the effects of motion. Several of these methods exist, including the inverse Gauss-Newton algorithm employed in this protocol, which minimizes the sum of squares cost function of the reference image and image under correction. The algorithm is useful because it enables fast and robust motion correction, using a GPU parallel platform design to reduce processing times[27].

For data reconstruction in this protocol, custom written software in a MATLAB environment was used for two-dimensional gridding reconstruction, where spiral samples are reconstructed in k-space into gridded images[31-33]. Time series data were generated by calculating the percent modulation of the BOLD signal of each voxel relative to the baseline period collected prior to stimulation. Voxels whose time series were synchronized to blocks of optogenetic stimulation with a coherence value of 0.35 or greater were defined as activated voxels; this coherence value corresponds to a less than 10^{-9} P value[8]. Coherence values were calculated as the magnitude of the Fourier transform at the frequency of repeated stimulation cycles divided by the sum-of-squares of all frequency components[8,27]. Familywise error can be controlled using the Bonferroni correction for multiple comparisons. Alternative methods of analysis can be used, including parametric statistical tests such as the general linear models (GLMs). The coherence method requires less prior knowledge of the HRF compared to the conventional general linear model. Therefore, it is advantageous when exploring data using ofMRI. However, the coherence method can only be used for data with block designs or selected event-related designs with a fixed interstimulus interval and may not be used in ofMRI data with other event-related designs or mixed designs. Subsequently, dynamic causal modeling (DCM) can be used to analyze interactions between brain regions identified through ofMRI. DCM is a Bayesian statistical technique developed for analysis of functional connectivity from system responses to experimental inputs during fMRI[34].

Additional technical concerns for ofMRI are discussed here. Implants can be damaged or fall off, leading to the removal of the affected animal from the study. Re-implantation surgeries are not recommended due to the additional uncertainty of targeting the same ROI as in the original implantation surgery and due to animal welfare issues. Because of the significant amount of time and resources invested into each animal subject, consideration of the strength of the material is a significant concern when choosing a suitable dental cement for use in ofMRI studies. The implantation surgery is a critical factor in maximizing the longevity of the implant and animal subject. For example, ensuring that the skull is dry before applying the dental cement and placing an adequate amount of cement around the ceramic ferrule implant can ensure stability over the potential months-long timeline of the animal during the study. Additionally, alternative cage designs can be explored and discussed with the local animal care facility to avoid cages with wire tops holding the food and water that often protrude into the cage and provide opportunities for the animal to damage the implant. Importantly, the dental cement must be chosen carefully to reduce artifacts that affect imaging and alternative cements can be tested by application onto a phantom and imaging in a scanner before use in animal experiments. Trial and error with various dental cements has shown that the cement used in this protocol gives relatively few artifacts. Another technical challenge in performing ofMRI is the accuracy of fiber optic placement at the intended ROI, given the extremely small distances that can exist between nuclei in the brain[35]. After

completing the implantation surgeries, T2-weighted anatomical scans can be used to determine correct placement by overlaying onto a brain atlas. The skill of the surgeon and practice performing these surgeries can improve correct placement rates. The specificity and expression of the opsin at the intended ROI can be verified at the conclusion of the study by perfusing the animal and fixing the brain, using immunohistochemistry or the endogenous fluorescence of a reporter-protein tagged to the opsin for visualization. These reporter proteins can also be colocalized with other proteins to ensure that the opsin is expressed in the desired neural cell types[1,8,15,25]. As mentioned previously, artifacts can arise when performing ofMRI due to tissue heating from light delivery[22]. The tissue heating causes modification of relaxation times, resulting in false BOLD signal. To ensure that activation resulting from light stimulation during ofMRI is not due to this artifact, opsin-negative controls should be performed in which either saline injected animals or animals injected with control fluorophore vectors (such as AAV-CaMKIIa-EYFP) undergo ofMRI. Additionally, only well-constructed fiber optic implants with good light transmission efficiency should be used to remove the need to use high laser powers. ofMRI studies have been performed in which false activation due to tissue heating has not been an issue[1,6-8,10,11].

Regarding the choice of vector to introduce the required optogenetic genes into neurons for expression, AAVs are not known to cause disease in humans and are therefore a convenient option, given the lower biosafety level required to use these agents (BSL-1). In addition, a multitude of vector cores carry AAVs packaged with various optogenetic genes in stock and with multiple serotypes. The serotype of AAV must be chosen based on the intended cell population target to ensure optimal expression levels[36,37]. Lentiviruses can also be used but require a higher biosafety level. The time period required for sufficient expression of the optogenetic genes is variable depending on the specific animal model used, on the particular AAV used and on the specific experimental paradigm. In this protocol, Sprague Dawley rats at 11 weeks old are used and optogenetic studies begin four to six weeks after virus injection. Transgenic mice can also be used in optogenetic studies. It is necessary to perform pilot experiments to determine the specific amount of time required for sufficient expression of the opsins. Stimulation paradigms can vary depending on the specific opsin used. In this protocol, AAV5-CaMKIIa-hChR2(H134R)-EYFP is used and the stimulation paradigm is 20 sec on/40 sec off. If using an SSFO, the stimulation paradigm will vary because the SSFO requires only a brief pulse of light to be activated and then a brief pulse of light at another wavelength to be terminated.

An additional critical concern when performing ofMRI is preventing light leakage from the ferrule implant interface with the fiber optic patch cable during optogenetic stimulation to prevent a confounding brain signal originating from visual stimulation, even when the animal is anesthetized. Cones of black electrical tape can be used to block the light from the ferrules and to cover the eyes of the animal. Importantly, physiological values including expiratory CO_2 and body temperature of the subject must be properly maintained throughout the duration of the imaging. Expiratory CO_2 should be kept between 3 - 4% and body temperature at 37 °C. In addition, the shimming sequences to reduce as much inhomogeneity as possible in the magnetic field prior to starting ofMRI scans greatly determines the quality of the resulting BOLD data. Control of these factors is critical in producing reliable ofMRI data. In this protocol, DPSS lasers are used as the light source for optogenetic stimulation. Because laser light is coherent, more than enough power can be easily supplied through the fiber optic. LED light sources coupled to fiber optics are available from commercial vendors, but have the disadvantage of decreased power of light transmission. The laser light source does require alignment to each particular fiber optic patch cable, but with practice, the alignment can be accomplished within seconds to minutes.

Future applications of ofMRI include the use of next-generation opsins such as red-shifted opsins to enable non-invasive stimulation during imaging. Additionally, the implantation of MRI-compatible EEG or similar recording electrodes along with the fiber optic implant could allow for the acquisition of high temporal resolution data in addition to the high spatial resolution data of MRI. ofMRI with electrophysiological recording could provide extensive information on the functional connectivity of the brain. In summary, the power of ofMRI to monitor the entire brain in response to the stimulation of specific cell populations defined by genetic or anatomical identity makes ofMRI a critical tool to use in the study of neurological diseases and of the connectomics of the healthy brain.

Disclosures

The authors have nothing to disclose.

Acknowledgements

References

1. Lee, J. H., *et al.* Global and local fMRI signals driven by neurons defined optogenetically by type and wiring. *Nature.* **465** (7299), 788-792 (2010).
2. Weitz, A. J., & Lee, J. H. Progress with optogenetic functional MRI and its translational implications. *Future Neurol.* **8** (6), 691-700 (2013).
3. Lee, J. H. Informing brain connectivity with optogenetic functional magnetic resonance imaging. *NeuroImage.* **62** (4), 2244-2249 (2012).
4. Lee, J. H. Tracing Activity Across the Whole Brain Neural Network with Optogenetic Functional Magnetic Resonance Imaging. *Front. Neuroinform.* **5** (October), 1-7 (2011).
5. Kahn, I., *et al.* Characterization of the Functional MRI Response Temporal Linearity via Optical Control of Neocortical Pyramidal Neurons. *J. Neurosci.* **31** (42), 15086-15091 (2011).
6. Takata, N., *et al.* Optogenetic Activation of CA1 Pyramidal Neurons at the Dorsal and Ventral Hippocampus Evokes Distinct Brain-Wide Responses Revealed by Mouse fMRI. *PLoS ONE.* **10** (3), e0121417 (2015).
7. Iordanova, B., Vazquez, A. L., Poplawsky, A. J., Fukuda, M., & Kim, S.-G. Neural and hemodynamic responses to optogenetic and sensory stimulation in the rat somatosensory cortex. *J. Cereb. Blood Flow Metab.* **35** (6), 922-932 (2015).

8. Weitz, A.J., *et al.* Optogenetic fMRI reveals distinct, frequency-dependent networks recruited by dorsal and intermediate hippocampus stimulations. *NeuroImage.* **107**, 229-241 (2015).

9. Desai, M., *et al.* Mapping brain networks in awake mice using combined optical neural control and fMRI. *J. Neurophysiol.* **105** (December 2010), 1393-1405 (2011).

10. Liang, Z., Watson, G. D. R., Alloway, K. D., Lee, G., Neuberger, T., & Zhang, N. Mapping the functional network of medial prefrontal cortex by combining optogenetics and fMRI in awake rats. *NeuroImage.* **117** (0), 114-123 (2015).

11. Byers, B., *et al.* Direct *in vivo* assessment of human stem cell graft-host neural circuits. *NeuroImage.* **114** (0), 328-337 (2015).

12. Boyden, E.S., Zhang, F., Bamberg, E., Nagel, G., & Deisseroth, K. Millisecond-timescale, genetically targeted optical control of neural activity. *Nat. Neurosci.* **8** (9), 1263-1268 (2005).

13. Carter, M.E., *et al.* Tuning arousal with optogenetic modulation of locus coeruleus neurons. *Nat. Neurosci.* **13** (12), 1526-1533 (2010).

14. Zhang, F., Wang, L.P., Boyden, E. S., & Deisseroth, K. Channelrhodopsin-2 and optical control of excitable cells. *Nat. Methods.* **3** (10), 785-792 (2006).

15. Zhao, S., *et al.* Cell type-specific channelrhodopsin-2 transgenic mice for optogenetic dissection of neural circuitry function. *Nat. Methods.* **8** (9), 745-752 (2011).

16. Ogawa, S., Lee, T. M., Kay, A. R., & Tank, D. W. Brain magnetic resonance imaging with contrast dependent on blood oxygenation. *Proc. Natl. Acad. Sci. U.S.A.* **87** (24), 9868-9872, (1990).

17. Ogawa, S., *et al.* Intrinsic signal changes accompanying sensory stimulation: functional brain mapping with magnetic resonance imaging. *Proc. Natl. Acad. Sci. U.S.A.* **89**, 5951-5955 (1992).

18. Kwong, K. K., Belliveau, J. W., *et al.* Dynamic magnetic resonance imaging of human brain activity during primary sensory stimulation. *Proc. Natl. Acad. Sci. U.S.A* **89**, 5675-5679 (1992).

19. Canals, S., Beyerlein, M., Murayama, Y., & Logothetis, N.K. Electric stimulation fMRI of the perforant pathway to the rat hippocampus. *Magn. Reson. Imaging.* **26**, 978-986 (2008).

20. Antal, A., *et al.* Imaging artifacts induced by electrical stimulation during conventional fMRI of the brain. *NeuroImage.* **85** (3), (2014).

21. Lin, J. Y., Knutsen, P. M., Muller, A., Kleinfeld, D., & Tsien, R. Y. ReaChR: a red-shifted variant of channelrhodopsin enables deep transcranial optogenetic excitation. *Nat. Neurosci.* **16** (10), 1499-508 (2013).

22. Christie, I. N., *et al.* FMRI response to blue light delivery in the naïve brain: Implications for combined optogenetic fMRI studies. *NeuroImage.* **66**, 634-641 (2013).

23. Aravanis, A.M., *et al.* An optical neural interface: *in vivo* control of rodent motor cortex with integrated fiberoptic and optogenetic technology. *J. Neural Eng.* **4**, S143-S156 (2007).

24. Pashaie, R., *et al.* Optogenetic brain interfaces. *IEEE Rev. Biomed. Eng.* **7**, 3-30 (2014).

25. Gradinaru, V., Mogri, M., Thompson, K. R., Henderson, J. M., & Deisseroth, K. Optical deconstruction of parkinsonian neural circuitry. *Science.* **324** (April), 354-359 (2009).

26. Rivard, A.L., *et al.* Rat intubation and ventilation for surgical research. *J. Invest. Surg.* **19**, 267-274 (2006).

27. Fang, Z., & Lee, J. H. High-throughput optogenetic functional magnetic resonance imaging with parallel computations. *J. Neurosci. Meth.* **218** (2), 184-195 (2013).

28. Da Silva, F.L. EEG: Origin and measurement. *EEG - fMRI: Physiological Basis, Technique, and Applications.* 19-38 (2010).

29. Becker, K., *et al.* Low dose isoflurane exerts opposing effects on neuronal network excitability in neocortex and hippocampus. *PLoS ONE.* **7** (6), 3-9 (2012).

30. Nishikawa, K., & Maciver, M. B. Agent-selective Effects of Volatile Anesthetics on GABA A Receptor - mediated Synaptic Inhibition in Hippocampal Interneurons. *Anesthesiology.* **94** (2), 340-347, (2001).

31. Jackson, J.I., Meyer, C.H., Nishimura, D.G., & Macovski, A. Selection of a convolution function for Fourier inversion using gridding. *IEEE Trans. Med. Imag.* **10** (3), 473-478 (1991).

32. Glover, G.H., & Lee, A.T. Motion artifacts in fMRI: comparison of 2DFT with PR and spiral scan methods. *Magn. Reson. Med.* **33** (20), 624-635 (1995).

33. Kim, D.H., Adalsteinsson, E., & Spielman, D.M. Simple analytic variable density spiral design. *Magn. Reson. Med.* **50**, 214-219 (2003).

34. Friston, K.J., Harrison, L., & Penny, W. Dynamic causal modeling. *Neuroimage.* **19**, 1273-1302 (2003).

35. Alkire, M.T., McReynolds, J.R., Hahn, E.L., & Trivedi, A.N. Thalamic microinjection of nicotine reverses sevoflurane-induced loss of righting reflex in the rat. *Anesthesiology.* **107** (2), 264-272 (2007).

36. Zincarelli, C., Soltys, S., Rengo, G., & Rabinowitz, J.E. Analysis of AAV serotypes 1-9 mediated gene expression and tropism in mice after systemic injection. *Mol. Ther.* **16** (6), 1073-1080 (2008).

37. Aschauer, D.F., Kreuz, S., & Rumpel, S. Analysis of Transduction Efficiency, Tropism and Axonal Transport of AAV Serotypes 1, 2, 5, 6, 8 and 9 in the Mouse Brain. *PLoS ONE.* **8** (9), 1-16 (2013).

38. Liu, J., *et al.* Frequency-selective control of cortical and subcortical networks by central thalamus. *eLife.* **4**, e09215 (2015).